Original Article

Direct assessment by electron spin resonance spectroscopy of the antioxidant effects of French maritime pine bark extract in the maxillofacial region of hairless mice

Ayaka Yoshida,[1,#] Fumihiko Yoshino,[1,#] Masahito Tsubata,[2,#] Motoya Ikeguchi,[2] Takeshi Nakamura[3] and Masaichi-Chang-il Lee[1,*]

[1]Department of Clinical Care Medicine, Division of Pharmacology and ESR Laboratories, Kanagawa Dental College, 82 Inaoka-cho, Yokosuka, Kanagawa 238-8580, Japan
[2]Toyo Shinyaku Co., Ltd., Research and Development Division, 7-28 Yayoigaoka, Tosu, Saga 841-0005, Japan
[3]Pharmacokinetics and Bioanalysis Center, Research Group 1, Research Department 1, Shin Nippon Biomedical Laboratories, LTD., Kainan Inteligence Park, 16-1 Minami Asakawa, Kainan, Wakayama 642-0017, Japan

(Received 2 August, 2010; Accepted 29 November, 2010; Published online 3 June, 2011)

Flavangenol, one of extract of French maritime pine bark, is a complex mixture of bioflavonoids with oligometric proanthocyanidins as the major constituents. These constituents, catechin and procyanidin B_1, are water-soluble derivatives of flavangenol. In this study, we investigated the antioxidant effects of flavangenol on reactive oxygen species such as hydroxyl radical, superoxide anion and singlet oxygen using electron spin resonance and spin trapping. The effect of flavangenol on oxidative stress in the skin from the maxillofacial region of hairless mice was investigated using an *in vivo* L-band electron spin resonance imaging system. Flavangenol attenuated oxidative stress in the maxillofacial skin by acting as a reactive oxygen species scavenger, as demonstrated by *in vitro* and *in vivo* electron spin resonance imaging analysis. The absorption and metabolism of flavangenol were also examined. After oral administration of flavangenol in human and rat, most of the catechin in plasma was in the conjugated form, while 45% to 78% of procyanidin B_1 was unconjugated, indicating that non-conjugated procyanidin B_1 would be active in the circulation. The ability of flavangenol to reduce reactive oxygen species levels in the circulation of the maxillofacial region suggests that this extract may be beneficial for skin protection from exposure to ultraviolet irradiation.

***Key Words*:** **reactive oxygen species, oxidative stress, electron spin resonance (ESR), antioxidants, French maritime pine bark extract**

Skin is a major target for toxic insult by a broad spectrum of physical (i.e. ultraviolet (UV) radiation) and chemical (xenobiotic) agents, which are capable of inducing structural and functional alterations. It is well known that skin is exposed to oxidative stress due to reactive oxygen species (ROS) such as hydroxyl radical ($HO^{\bullet}$), superoxide ($O_2^{\bullet-}$) and singlet oxygen ($^1O_2$), which originate exogenously and in the skin itself.[1] Administration of antioxidant has been investigated as a means to prevent or treat ROS-mediated cellular injury and thereby restore homeostasis in the skin.[2,3] Although many antioxidants have shown considerable efficacy in the cell culture systems and in the animal models of oxidative injury, unequivocal confirmation of the beneficial effects of antioxidant therapy in human has proven elusive.[1,4]

The antioxidant effects of French maritime pine bark extract against ROS-induced tissue injury are well known.[5,6] Flavangenol (FVG), one trade name of pine bark extract, is a unique mixture of bioflavonoid consisting mainly of monomers ([+]-catechin and epicatechin) and condensed falconoid known as proanthocyanidins (Fig. 1). Treatment with FVG has been shown to reduce ischemia/reperfusion-induced renal injury and to exert protective effects against endothelial dysfunction.[7,8] Furthermore, FVG have been shown to prevent or attenuate atherosclerosis and diabetes.[9,10]

We previously developed an electron spin resonance (ESR)-based technique for the detection of ROS in biological systems.[11–17] Nitroxyl radicals are very useful as an exogenous spin probes for measuring free radical distribution, oxygen concentration and redox metabolism by *in vivo* ESR in biological systems.[14–18] It has been reported that nitroxyl radicals, referred to as a 'nitroxyl spin

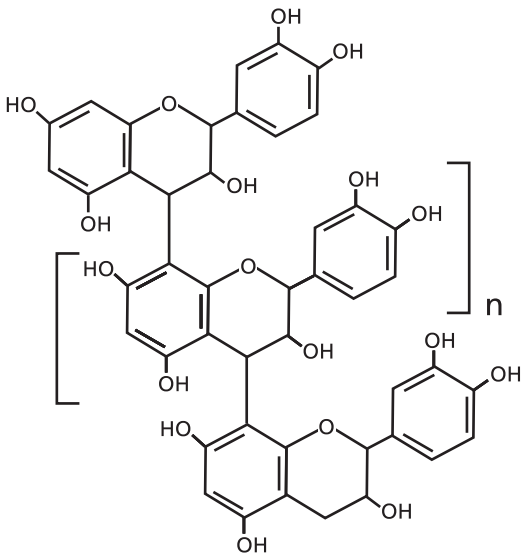

Fig. 1. Structure of oligometric proanthocyanidins, the major constituents of FVG.

*To whom correspondence should be addressed.
E-mail: ieeman@kdcnet.ac.jp
#These authors contributed equally to this work.

doi: 10.3164/jcbn.10-103

probes', lose their paramagnetism through a redox reaction when exposed to a reducing agent in biological systems.[19,20] The signal decay rate of the nitroxyl spin probe provides evidence of ROS generation and changes of redox status in biological systems.[21,22]

The hairless mouse has been used in studies investigating oxidative stress induced by UV irradiation.[23,24] The first study to utilize the L-band ESR technique demonstrated that ROS were generated in response to visible light-irradiation of the skin of mice in a protoporphyria model.[25] The study compared ESR imaging of the head region in live mice and isolated rat brain using the blood brain barrier (BBB)-permeable nitroxyl spin probe, 3-methoxycarbonyl-2,2,5,5-tetramethylpyrrolidine-1-oxyl (MC-PROXYL) or the blood-brain-barrier impermeable probe 3-carbamoyl-2,2,5,5-tetramethylpyrrolidine-1-oxyl (carbamoyl-PROXYL; C-PROXYL).[16] The results showed C-PROXYL was widely distributed in the maxillofacial region, but not in the brain. Thus, the L-band ESR imaging technique was subsequently used with the nitroxyl spin probe C-PROXYL for the assessment of oxidative stress in the maxillofacial region of hairless mice. In the present study, we used the ESR technique to investigate the ROS scavenging effect of FVG and the decay rate constant of C-PROXYL in the maxillofacial region of hairless mice. In addition, we investigated the absorption and metabolism of FVG in plasma following administration in rat and human. The results of *in vitro* and *in vivo* ESR imaging analysis showed that administration of FVG to hairless mice was capable of reducing ROS-mediated oxidative stress in the circulation of the maxillofacial region due to a direct ROS-scavenging effect.

Materials and Methods

Reagents. FVG used in this study was supplied by Toyo Shinyaku Co., Ltd. (Saga, Japan). The FVG consisted of 72.5% polyphenol (determined by the Folin-Denis method) with 5 procyanidin B_1 (PB_1), 2.98% catechin, and 0.23% epicatechin. PB_1 was purchased from Tokiwa Phytochemical Co., Ltd. (Chiba, Japan). C-PROXYL, xanthine oxidase (XO), and xanthine were purchased from Sigma-Aldrich (St. Louis, MO). Catechin, epicatechin, methanol and acetonitrile (HPLC grade); acetic acid, formic acid, propylene glycol, sodium acetate (special reagent grade); hydrogen peroxide (H_2O_2), ferrous sulfate heptahydrate ($FeSO_4$), 2,2,6,6-tetramethyl-4-piperidone (4-oxo-TEMP), and rose bengal were purchased from Wako Pure Chemical Industries (Osaka, Japan). 4H-EDTA (free acid) was supplied by Dojindo Laboratories (Kumamoto, Japan). 5-(2,2-dimethyl-1,3-propoxy-cyclophosphoryl)-5-methyl-1-pyrroline-*N*-oxide (CYPMPO) was purchased from Radical Research (Tokyo, Japan). Pentobarbital sodium was purchased from Kyoritsu Seiyaku Corporation (Tokyo, Japan).

***In vitro* ESR measurement.** $HO^{\bullet}$ was generated by the Fenton reaction (H_2O_2 plus $FeSO_4$) as described previously.[17] $O_2^{\bullet-}$ was generated by the xanthine-XO system also described previously.[17] We verified the generation of $^1O_2$ by the photochemical reaction of rose bengal illuminated for 2 min (18,000 lux) using an ESR technique with 4-oxo-TEMP as a $^1O_2$ spin trap.[26,27] All solutions were prepared in ultra-pure water. ESR spin trapping was conducted with a ROS-generating system containing CYPMPO[28] or 4-oxo-TEMP[26,27] as the spin trap. ESR observations were performed with a JES-RE1X, X-band spectrometer (JEOL, Tokyo, Japan) connected to a WIN-RAD ESR Data Analyzer (Radical Research, Tokyo, Japan) at the following instrument settings: microwave power, 8.00 mW; magnetic field, 335.5 ± 5–7.5 mT; field modulation width, 0.079–0.1 mT; receiver gain, 125–400; sweep time, 1 min; and time constant, 0.03 s. For each experiment, the effects of all compounds were calculated and represented as percent of the mean control value as 100%, respectively.

Animals and *in vivo* ESR experimental design. The procedures used in this study were in accordance with the guidelines of the US National Institute of Health Guide for the Care and Use of Laboratory Animals (NIH Publication No. 85–23, revised 1985) and the protocols were approved by the Animal Care Committees (Yokosuka, Japan). 5-weeks-old female HR-1 hairless mice were purchased from Japan SLC (Shizuoka, Japan). Animals were housed in a light-controlled room with a 12-h light/dark cycle and were allowed *ad libitum* access to food and water. FVG (200 or 600 mg/kg body weight/day) were administered orally for 4 days. From days 2 to 4, the mice were exposed to UVB irradiation (emission: 280–315 nm, 10 min; 0.1 mW; SUPERCURE-203S, RU-340, Radical Research, Tokyo, Japan, Fig. 2). At day 5, the mice were anesthetized with pentobarbital sodium (50 mg/kg, *i.p.*) and the maxillofacial region was subsequently analyzed by *in vivo* L-band ESR using C-PROXYL as the spin probe, as described previously.[16,25]

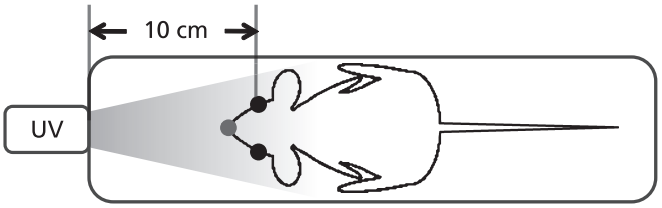

Fig. 2. Experimental setup in the maxillofacial region of hairless mice exposed to UVB irradiation.

In vivo ESR-CT imaging system constructed in our laboratory and JEOL ESR application laboratory was used.[14–16] This system consists of a commercially available electromagnet (modified RE3X, JEOL, Tokyo, Japan), a pair of field scan coils, power supplies, a personal computer, and a 1-GHz microwave unit containing a four-window loop-gap resonator (28 × ϕ43 mm, the measurement position centered on the eyeball). The system is provided with four different coil sets, three for the gradients (0.9 mT/cm, max) and one for rapid scanning. The gradient field was controlled by a current stabilizer, which is controlled by a personal computer (Dell Precision PWS 380).

The ESR-CT images were constructed on the basis of Lauterbur's method,[29] known as a 3D zeugmatography. We applied linear magnetic field gradients along the *x*-, *y*-, and *z*-axes produced by the magnetic field gradient coils. For the 2D imaging, 36 projections alternating between gradient and nongradient were acquired in 55 s. Each projection required 1024 points of acquisition data for imaging. The ESR absorption spectra were obtained by integrating the derivative spectrum with the recorded gradient. The mid-field hyperfine line in the spectrum was separated from the triplet signal of the nitroxyl radicals. Each signal data set was convoluted with Shepp's filter function into the Fourier domain before performing the inverse Fourier transformation to the spatial domain. The 2D imaging pictures of 512 × 512 points were obtained from 18 projections for gradient step at 10° in the spatial domain. Instrument settings for ESR detection of C-PROXYL were as follows: microwave power, 20 mW; magnetic field, 31.0–34.0 ± 1.0 mT; field modulation width, 0.1 mT; receiver gain, 63–125; time constant, 0.01 s: field intensity, 0.7 mT/cm.

Pharmacokinetic studies. Human pharmacokinetic experiments were performed in seven healthy male volunteers, aged 25 to 41 y (mean, 29.1 y). They had been fully informed of the nature of the experiment and of the study protocol. 2 days before administration, the subjects were provided with a polyphenol-restricted diet. Blood samples were collected at 0, 2, 4, 6, and 24 h after oral administration of 5 g FVG dissolved in 100 ml water. Plasma was obtained by centrifugation (3,000 rpm) of blood samples. 6-weeks-old male Wistar rats (CLEA Japan Inc., Tokyo, Japan) were housed at 22 ± 3°C and 50 ± 20% humidity under a 12 h light/dark

doi: 10.3164/jcbn.10-103

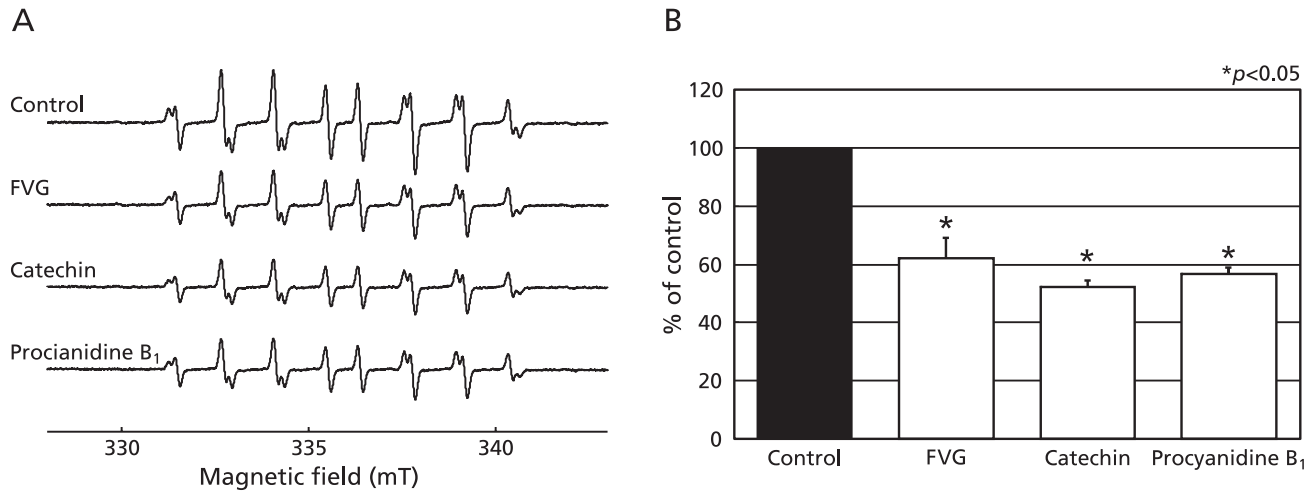

Fig. 3. Effects of FVG, PB_1 and catechin on $HO^{\bullet}$ generation *via* the Fenton reaction. A, ESR spin trapping measurement of $HO^{\bullet}$ generation by H_2O_2 (20 μM) and $FeSO_4$ (20 μM) in 0.1 M PBS (pH 7.2) with CYPMPO (5 mM) as the spin trap (a) in the absence of antioxidant; FVG (b; 100 μg/ml), catechin (c; 100 μg/ml) and PB_1 (d; 100 μg/ml), respectively. B, the effects of FVG, catechin and PB_1 on $HO^{\bullet}$ generation from the Fenton reaction. The signal intensity of the seventh peak of the spectrum was normalized as the relative height against the signal intensity of control. Results are expressed as percent of control and are represented as mean ± SEM. * indicates a significant difference (p<0.05) versus the corresponding control value.

cycle. After habituation for 1 week, the rats were fasted overnight and treated orally with 600 mg/kg FVG in 20 ml of distilled water *via* gastric incubation. Blood samples were collected at 0, 1, 2, 4 and 24 h after FVG administration.

Preparation of standard and reagent solutions for liquid chromatography/mass spectrometry/mass spectrometry (LC/MS/MS). PB_1 stock standard solution (100 μg/ml) and catechin stock standard solution (100 μg/ml) were prepared by dissolving the compounds in ultra-pure water with further dilution for a calibration curve at concentration of 5,000, 2,500, 1,000, 500, 250, 100, 50 ng/ml, and for quality control (QC) samples at concentration of 4,000, 2,000, 100, 50 ng/ml. Epicatechin stock internal standard (IS) solutions (100 μg/ml) were prepared in methanol and diluted to a concentration of 500 ng/ml. Sodium acetate (4.1 g) and 4H-EDTA free acid (0.5 g) were dissolved in and diluted with 500 ml of ultra-pure water. The resultant solution was adjusted to pH 5.0 by adding acetic acid to make Lys Buffer.

LC/MS/MS analysis. The Shimadzu 10A HPLC system (Shimadzu Co., Ltd., Kyoto, Japan) and API4000 system (MSMS system, Applied Biosystems, Foster, CA) were used for the LC/MS/MS analysis. The analytical column was a Cadenza CD-C18 (2.0ϕ × 150 mm, S-3, Imtakt Inc., Kyoto, Japan). The column temperature was maintained at 40°C. Sample temperature was stored at room temperature. The flow rate was 0.2 ml/min and a gradient analysis of mobile phase A (0.1% formic acid) and phase B (acetonitrile) was performed according to the next time program (0 to 20 min, mobile phase A at 95% to 25%; 20.01 to 25 min, mobile phase A at 20%; 25.01 to 30 min, mobile phase A at 95%).

Turbo ionspray was used in negative ion mode (heater temperature; 400°C). The mass was from *m/z* 577 to 289 for PB_1, 289 to 245 for catechin, and 441 to 169 for IS in multiple reaction monitoring (MRM) scan mode. Unconjugated PB_1, unconjugated catechin, total PB_1, and total catechin were removed according to pretreatment methods and quantified simultaneously. Calibration of the samples and blank sample were treated as one set and analyzed by the analytical method. A calibration curve (weighting factor: $1/X^2$) was constructed by least squares linear regression using the peak area ratios. Concentration was determined by comparing the peak area ratios of samples with those from the calibration curve. Samples expected to exceed the upper limit of the calibration curve were analyzed after dilution with control plasma or serum.

Statistical analysis. Tukey multiple comparison test was used to compare averages between control and FVG groups. p value less than 0.05 was considered to be statistically significant.

Results

Effects of FVG on $HO^{\bullet}$ generation by the Fenton reaction. In the present study, the effect of FVG on $HO^{\bullet}$ generated by the Fenton reaction was assessed using ESR and spin trapping with CYPMPO. In agreement with our previous report,[28] we observed that the combination of H_2O_2 and $FeSO_4$ (Fenton reagent) in the presence of CYPMPO led to the formation of a characteristic CYPMPO-OH spin adduct spectrum with hyperfine splitting giving rise to 14 resolved peaks (Fig. 3A). When the reaction mixtures were pretreated with FVG, catechin or PB_1 in the presence of $FeSO_4$ and H_2O_2 was subsequently added, the CYPMPO-OH signal intensity was reduced (Fig. 3A). These data indicate that, within our experimental system, FVG, catechin, and PB_1 markedly inhibited $HO^{\bullet}$ generation from the Fenton reaction (Fig. 3B).

Effects of FVG on $O_2^{\bullet-}$ generation from xanthine/XO system. We also investigated the effects of FVG on $O_2^{\bullet-}$ generation from XO system, as measured by ESR spin trapping with CYPMPO. In agreement with our previous findings,[28] addition of xanthine to XO led to the formation of a characteristic CYPMPO-OOH spin adduct spectrum with hyperfine splitting giving rise to 14 resolved peaks (Fig. 4A). When similar reaction mixtures were pretreated with FVG, catechin or PB_1, the CYPMPO-OOH signal intensity was reduced (Fig. 4A). These data indicated that FVG, catechin, and PB_1 markedly inhibit $O_2^{\bullet-}$ generated by the xanthine/XO system (Fig. 4B).

Effects of FVG on the generation of $^1O_2$ by illuminated rose Bengal. In our final experiment, we examined the effects of FVG on $^1O_2$ generated from illuminated rose bengal, as measured by the ESR spin trapping with 4-oxo-TEMP. The characteristic ESR spectrum pattern of 3 equal-intensity lines of the 4-oxo-TEMPO radical, indicative of $^1O_2$ generation,[26,27] was observed when rose bengal was illuminated for 2 min in the presence of 4-oxo-TEMP (Fig. 5A). Catechin and PB_1 inhibited the ESR signal intensity of the 4-oxo-TEMPO radical, while FVG had no significant change (Figs. 5 A and B).

ESR Imaging Assessment of Oxidative Stress in the maxillofacial region of hairless mice. C-PROXYL is a suit-

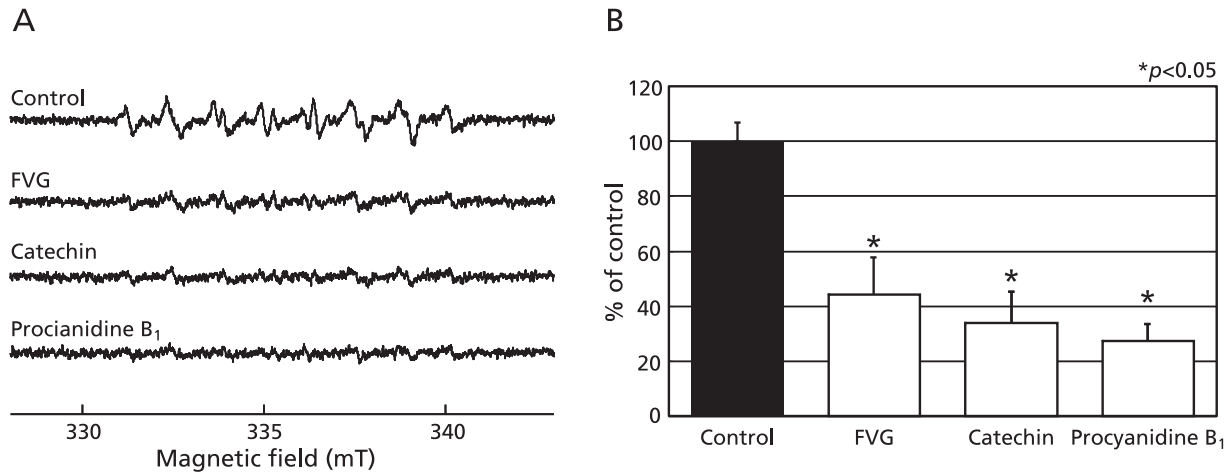

Fig. 4. Effects of FVG, PB_1 and catechin on $O_2^{\bullet-}$ generated by xanthine-XO system. A, ESR spin trapping measurement of $O_2^{\bullet-}$ generation by xanthine (1 mM) and XO (0.5 U/ml) in distilled water with CYPMPO (10 mM) as the spin trap (a) in the absence of antioxidant; FVG (b; 100 μg/ml), catechin (c; 100 μg/ml), and PB_1 (d; 100 μg/ml), respectively. B, the effects of FVG, catechin, and PB_1 on $O_2^{\bullet-}$ generated by xanthine-XO. The signal intensity of the seventh peak of the spectrum was normalized as the relative height against the signal intensity of a control. Results are expressed as percent of control and are represented as mean ± SEM. * indicates a significant difference (p<0.05) versus the corresponding control value.

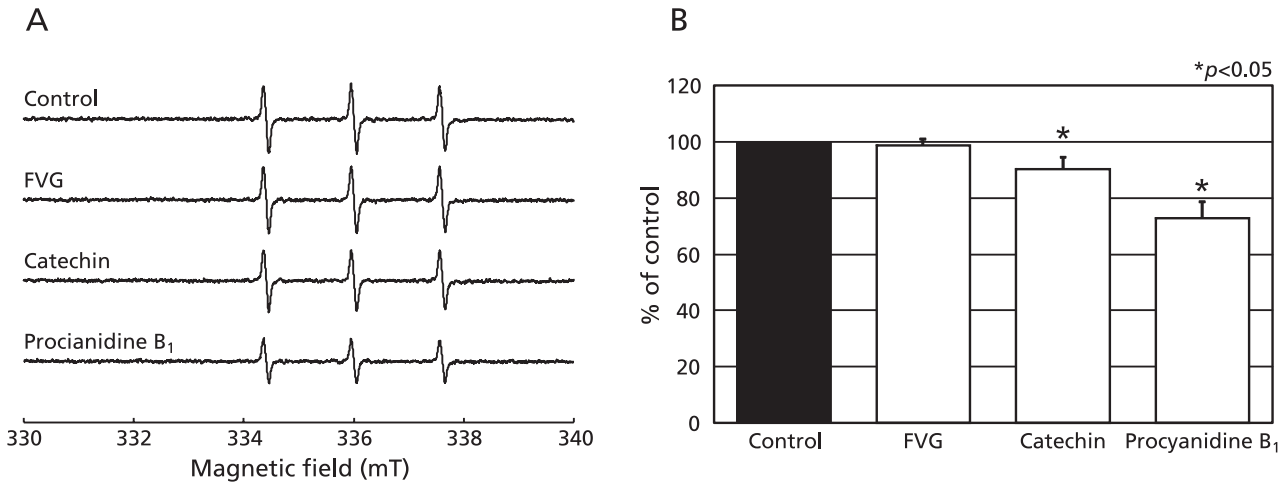

Fig. 5. Effects of FVG, PB_1 and catechin on $^1O_2$ generated by illuminated rose bengal. A, ESR spin trapping measurement of $^1O_2$ produced by the photochemical reaction of rose bengal illuminated for 2 min (18,000 lux) with 4-oxo-TEMP (40 mM) as the spin trap (a) in the absence of antioxidant; control with FVG (b; 100 μg/ml), catechin (c; 100 μg/ml), and PB_1 (d; 100 μg/ml) pre-treatment, respectively. B, the effects of FVG, catechin, and PB_1 on $^1O_2$ generated by illuminated rose bengal. The signal intensity of the second peak of the spectrum was normalized as the relative height against the signal intensity of a control. Results are expressed as percent of control and are represented as mean ± SEM. * indicates a significant difference (p<0.05) versus the corresponding control value.

able spin probe for the study of free radical reactions in the rodent skin by *in vivo* ESR detection.[16,25] These methods were also applied for the imaging of the maxillofacial region of hairless mice. In ESR studies of the maxillofacial region of hairless mice after *i.v.* treatment with C-PROXYL, we initially assessed the distribution of C-PROXYL from 2D projections of the sagittal section (*z-x* plane) (Fig. 6). Fig. 6 shows the time-dependent change of the ESR image of C-PROXYL in the maxillofacial region of hairless mice. These ESR images show that the decay of C-PROXYL in pretreatment of UVB-irradiated mice was faster than in control (Figs. 6 A and B). These findings suggest that oxidative stress induced by UVB irradiation, which has been reported previously in hairless mice, was responsible for the altered decay rate of C-PROXYL in the maxillofacial region. Pretreatment of UVB-irradiated mice with high-dose FVG (600 mg/kg) seemed to normalize the decay of C-PROXYL (Fig. 6D), but this effect was not observed at the lower dose (200 mg/kg) of FVG (Fig. 6C).

Effects of FVG on UV-induced oxidative stress in the maxillofacial region of hairless mice. To confirm the data from the ESR imaging experiments, we performed *in vivo* L-band ESR analysis with C-PROXYL under the same conditions, and the effect of FVG on UV-induced oxidative stress in the maxillofacial region of hairless mice was determined. The metabolism of C-PROXYL in the maxillofacial region of hairless mice can be divided into phase I and phase II, according to a two-compartments model of distribution (Fig. 7).[16,17] The decay rate constant of C-PROXYL was significantly greater in the maxillofacial region of UVB-irradiated hairless mice (Fig. 7A). Pretreatment of UVB-irradiated mice with high-dose FVG (600 mg/kg) resulted in

doi: 10.3164/jcbn.10-103

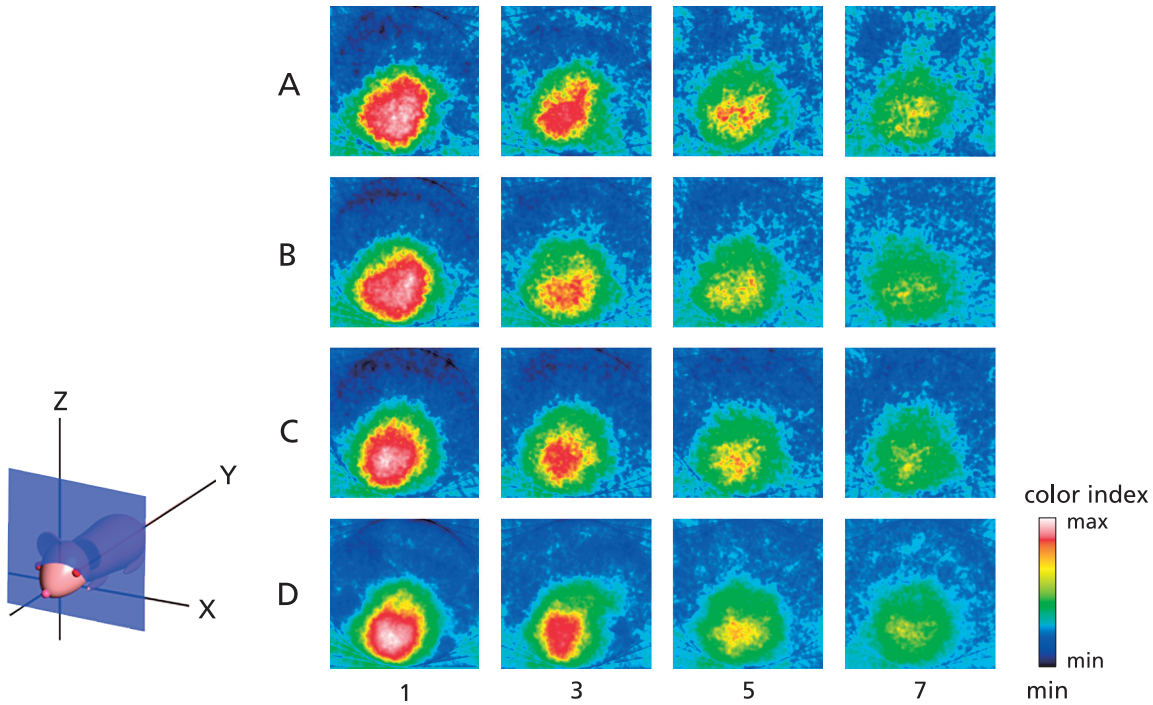

Fig. 6. 2D ESR projection images (*z-x* plane) of C-PROXYL distributions in the maxillofacial region of hairless mice. The ESR was measured at 1, 3, 5 and 7 min after *i.v.* treatment with C-PROXYL. A; control (non-UVB irradiation); B; UVB irradiation; C; 200 mg/kg or D; 600 mg/kg FVG pretreatment for 4 days with UV irradiation, respectively. As indicated by the attached color scale (32 colors; white and 100 being the maximum ESR signal), ESR images were reproduced in 32 colors and signals lower than 10% of the maximal signal intensity detected in all slices were regarded as noise. Experimental conditions were as described under "Methods".

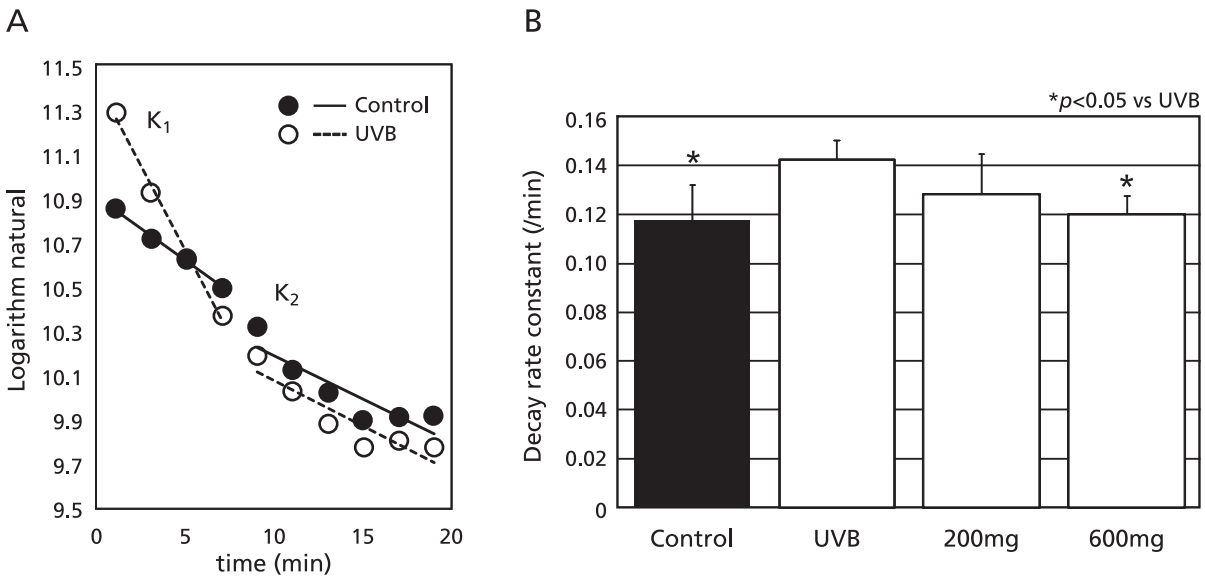

Fig. 7. Effects of FVG on UVB-induced oxidative stress in the maxillofacial region of hairless mice. Mice were anesthetized with pentobarbital sodium (50 mg/kg, *i.p.*). L-band ESR was used to determine the signal decay of C-PROXYL in the maxillofacial skin of hairless mice. A, Decay rate constants of (K_1 and K_2) of C-PROXYL after UVB irradiation (open circle); control (non-UVB irradiation, closed circle). B, the columns represent: K_1 of C-PROXYL after UVB irradiation, control (non-UVB irradiation); UVB irradiation with FVG (200 mg/kg or 600 mg/kg) pretreatment for 4 days respectively. The results are expressed as mean ± SD of hairless mice (n = 7). * indicates a significant difference (p<0.05) versus the corresponding value in control group.

a significant decrease in the decay rate constant of C-PROXYL, however the effect of FVG at the lower dose (200 mg/kg) was not significant (Fig. 7B).

The pharmacokinetics of FVG in rat and human plasma. The pharmacokinetics of the metabolites of FVG, PB_1, and catechin in plasma were determined by LC/MS/MS. Fig. 8A

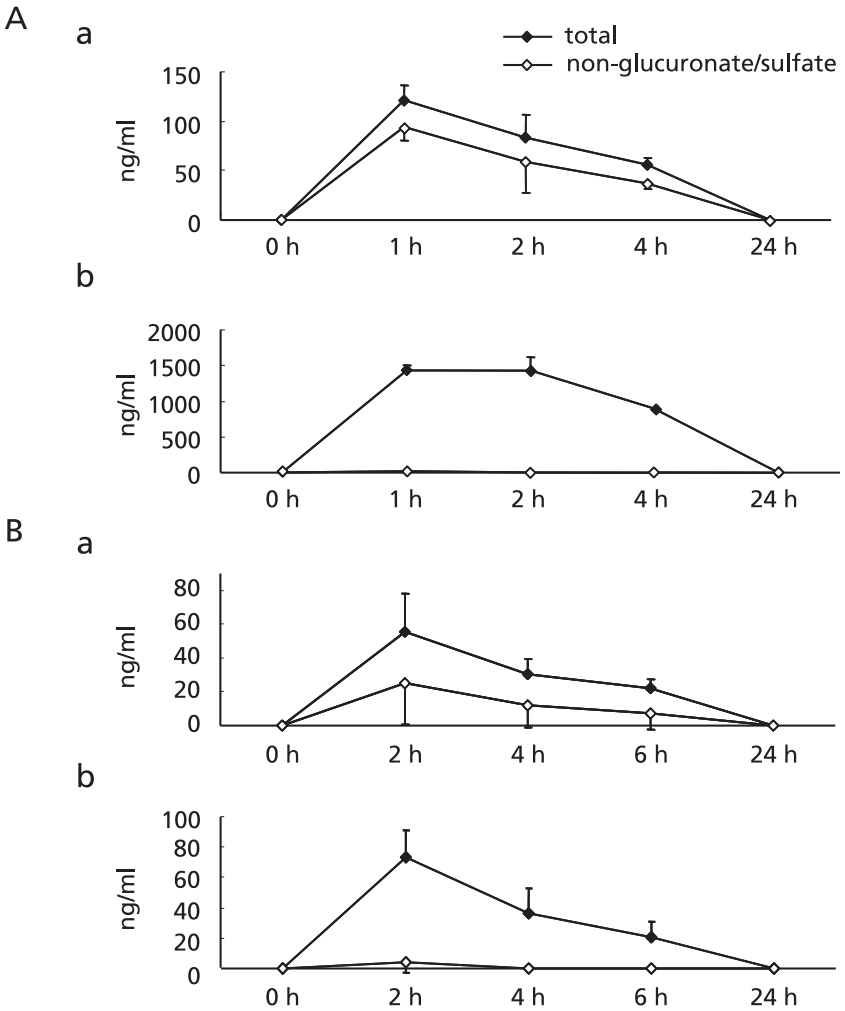

Fig. 8. Alteration in the concentration of PB_1 and catechin in rat serum and human plasma following oral administration of FVG. A, Changes in the plasma concentration of PB_1 and catechin in rats. FVG was given to rats (n = 5) by oral administration (600 mg/kg). Mean concentration of total (closed rhombus) and non-glucuronate/sulfate–conjugated (open rhombus) PB_1 (a) and catechin (b) in serum. B, Changes in the plasma concentration of PB_1 and catechin in human subjects. FVG (5 g) with 100 ml water was given to subjects (n = 6–7). Mean of total (closed rhombus) and non-glucuronate/sulfate–conjugated (open rhombus) PB_1 (a) and catechin (b) in plasma.

shows changes over time in the total concentration and the concentration of non-glucurono/sulfo–conjugated metabolites of PB_1 and catechin in rat serum. After oral administration of FVG, PB_1 and catechin were detected at 1, 2, 4 and 24 h. The highest PB_1 and catechin concentrations were reached between 1 h to 2 h. The concentration of non-conjugated PB_1 after administration of FVG was higher than that of catechin throughout the experimental period, except at 24 h. Fig. 8B shows the total concentration of PB_1 and catechin, and the concentration of their non-glucurono/sulfo–conjugated metabolites in human plasma. After oral administration of FVG, PB_1 and catechin were detected at 2, 4, 6 and 24 h. In human plasma, as in rat serum, there was a non-significant trend for non-conjugated PB_1 to be present at higher concentrations than non-conjugated catechin.

Discussion

There has been growing interest in harnessing the biologic activity of plant extracts such as pycnogenol obtained from the bark of the French maritime pine (*Pinus maritime*). Pycnogenol protects against oxidative stress in several experimental systems by doubling the intracellular synthesis of antioxidant enzymes and by acting as a potent ROS scavenger.[5,6] It has been reported that FVG, which is also extracted from the bark of the French maritime pine, exerts antioxidant effects in animal models of ROS-induced diseases.[7,8,10] However, these previous studies failed to demonstrate direct scavenging effects of FVG on ROS. Consequently, we undertook the present ESR study to assess the scavenging effects of FVG on ROS. The results of the study provide evidence that FVG inhibits $HO^{\bullet}$ and $O_2^{\bullet -}$ (Figs. 3 and 4).

Furthermore, we showed that catechin and PB_1, which are two of the major constituents of FVG, also reduced ROS such as $HO^{\bullet}$, $O_2^{\bullet -}$ and $^1O_2$ (Figs. 3–5), indicating that the compounds act as an antioxidants. Additional studies are needed to determine the precise mechanism by which catechin and PB_1 scavenge ROS *in vitro* and in the maxillofacial region of hairless mice *in vivo*.

The antihypertensive effect of FVG is attributable to both its antioxidant-mediated protective effect against endothelial dysfunction and its endothelium-dependent vasorelaxant effect, which is mediated by endothelial nitric oxide synthase activation.[7] However, there is little evidence about the potential *in vivo* effects of FVG on oxidative stress in specific organ systems, such as skin. *In vivo* L-band ESR spectroscopy and ESR imaging system is a highly useful technique for the non-invasive investiga-

doi: 10.3164/jcbn.10-103

tion of redox status in living organisms. Several previous studies have demonstrated that quantitative ESR analysis using the spin probe C-PROXYL, a blood-brain-barrier impermeable probe, can be used to investigate redox status under conditions of oxidative stress in the skin of the maxillofacial region in mice.[15,16,25] Hairless mice have been previously used to study oxidative stress resulting from irradiation.[23,24] It is known that UVB light is absorbed in the epidermis and but does not readily permeate subcutaneous tissue.[30] Inflammatory cells were not observed in subcutaneous tissue of skin samples from hairless mice, which had been collected immediately after the L-band ESR measurement and stained with hematoxylin and eosin (data not shown). Therefore, it appears that the skin was the main region measured by the L-band ESR technique in the present study. The results of *in vivo* ESR imaging and L-band ESR in UVB-irradiated hairless mice the present study indicate that the ESR technique in general, and in particular the ESR imaging technique employed herein, could be a powerful tool to selectively detect free radicals and to monitor free radical reactions *in vivo* in the skin of the maxillofacial region of mice (Figs. 5 and 6). Furthermore, the experiments confirmed that ESR imaging and L-band ESR are highly useful for the *in vivo* assessment of the antioxidant properties of functional foods (Figs. 5 and 6). The decay rate constant of C-PROXYL decreased when animals were pretreated with FVG at a dose of 600 mg/kg but not at 200 mg/kg (Figs. 6 C, D and 7B). When hairless mice were pretreated with FVG at 600 mg/kg prior to UVB irradiation, the level of oxidative stress in the maxillofacial skin was comparable to that seen in non-irradiated mice. Therefore, FVG might be useful as an antioxidant for the prophylaxis of ROS-induced skin diseases.

In a previous study using L-band ESR analysis, we reported that the metabolism of lipophilic nitroxyl spin probes in the brain can be divided into phase I (vascular system) and phase II (reduced excretion *via* the kidney), according to a two-compartment model of distribution.[15–17] The present study indicated that the metabolism of C-PROXYL in the maxillofacial region of hairless mice also occurred according to a two-compartment model (K_1 and K_2; Fig. 7A). The metabolism of C-PROXYL probably occurred mainly during phase I because of the presence of ascorbic acid, which is a strong reducing agent of nitroxyl spin probes in the vascular system of the maxillofacial skin.[16,17] These results suggest that FVG may reduce UVB-induced oxidative stress by scavenging ROS in the circulation of the maxillofacial region, and that the K_1 of C-PROXYL reflected oxidative stress induced by ROS in the vasculature.

PB_1, a water-soluble derivative of FVG, has been shown to exhibit the same biological activities as catechin *in vitro*, but the properties of this compound in the human body remain to be fully elucidated. In this study, we compared the metabolic fate and the bioavailability of PB_1 and catechin in both rat serum and human plasma. Following administration of FVG, most of the catechins were in the glucurono/sulfo-conjugated form in the plasma of both species. Conversely, 45% to 78% of PB_1 was present in the non-conjugated form in plasma. It should be noted that non-conjugated PB_1 was detected both human plasma and rat serum. Thus, a high percentage of glucurono/sulfo-conjugated PB_1 in plasma or serum is metabolized following oral administration of FVG, suggesting that non-conjugated PB_1 may contribute to the biological activity of FVG. In terms of human applications for our results, it is important to consider the relative concentration of the FVG used in the present study. Following administration of FVG (5 g/100 ml), the maximum plasma concentrations was 60 ng/ml for PB_1, and 80 ng/ml for catechin (Fig. 8B), compared to the concentration of FVG of 100 μg/ml used in our *in vitro* experiments (Figs. 3–5). It is possible that the scavenging effects of FVG, which is often used in *in vitro* studies, may reach the plasma. The redox potential of unchanged FVG and FVG metabolites that reach the plasma enables them to scavenge damaging radicals, but endogenous plasma antioxidants, especially ascorbate, are required for disposal of the resultant phenoxyl radicals.[31] The concentration of ROS in *in vitro* experiments would likely be much higher than concetrations *in vivo*, such as in human plasma. The maxillofacial skin from hairless mice undergoes oxidative stress in response to UV irradiation.[23,24] The results of the present study show that the higher concentration FVG normalized oxidative stress in the in maxillofacial skin of hairless mice (Figs. 6 C, D and 7B). These results suggest that FVG may have potentially beneficial antioxidant effects *in vivo* in humans. However, further studies are needed to evaluate the effect of FVG up UV-induced skin disease.

In conclusion, the present study demonstrated that FVG exhibits antioxidant properties by scavenging ROS, and that it may reduce oxidative stress induced by UVB irradiation in the skin of the maxillofacial region of hairless mice. These results suggest that FVG might be able to prevent ROS-related skin diseases, such as photo-aging. Furthermore, Quantitative ESR imaging analysis using C-PROXYL will be useful for understanding redox status under conditions of oxidative stress in the skin of the maxillofacial region of hairless mice.

Acknowledgments

This work supported by Toyo Shinyaku Co., Ltd. and by grants from High-Tech Research Center Project of Kanagawa Dental College, Yokosuka, Kanagawa.

Abbreviations

C-PROXYL	3-carbamoyl-2,2,5,5-tetramethylpyrrolidine-1-oxyl, carbamoyl-PROXYL
CYPMPO	5-(2,2-dimethyl-1,3-propoxycyclophosphoryl)-5-methyl-1-pyrroline-*N*-oxide
ESR	electron spin resonance
$FeSO_4$	ferrous sulfate heptahydrate
FVG	Flavangenol
H_2O_2	hydrogen peroxide
$HO^{\bullet}$	hydroxyl radical
IS	internal standard
LC/MS/MS	liquid chromatography/mass spectrometry/mass spectrometry
MC-PROXYL	3-methoxycarbonyl-2,2,5,5-tetramethylpyrrolidine-1-oxyl
MRM	multiple reaction monitoring
$^1O_2$	singlet oxygen
$O_2^{\bullet -}$	superoxide
4-oxo-TEMP	2,2,6,6-tetramethyl-4-piperidone
PB_1	procyanidin B_1
QC	quality control
ROS	reactive oxygen species
UV	ultraviolet
XO	xanthine oxidase

References

1 Trouba KJ, Hamadeh HK, Amin RP, Germolec DR. Oxidative stress and its role in skin disease. *Antioxid Redox Signal* 2002; **4**: 665–673.

2 Katiyar SK. Skin photoprotection by green tea: antioxidant and immunomodulatory effects. *Curr Drug Targets Immune Endocr Metabol Disord* 2003; **3**: 234–242.

3 Vayalil PK, Mittal A, Hara Y, Elmets CA, Katiyar SK. Green tea polyphenols prevent ultraviolet light-induced oxidative damage and matrix metalloproteinases expression in mouse skin. *J Invest Dermatol* 2004; **122**: 1480–

1487.
4 Bickers DR, Athar M. Oxidative stress in the pathogenesis of skin disease. *J Invest Dermatol* 2006; **126**: 2565–2575.
5 Packer L, Rimbach G, Virgili F. Antioxidant activity and biologic properties of a procyanidin-rich extract from pine (Pinus maritima) bark, pycnogenol. *Free Radic Biol Med* 1999; **27**: 704–724.
6 Rohdewald P. A review of the French maritime pine bark extract (Pycnogenol), a herbal medication with a diverse clinical pharmacology. *Int J Clin Pharmacol Ther* 2002; **40**: 158–168.
7 Kwak CJ, Kubo E, Fujii K, and *et al*. Antihypertensive effect of French maritime pine bark extract (Flavangenol): possible involvement of endothelial nitric oxide-dependent vasorelaxation. *J Hypertens* 2009; **27**: 92–101.
8 Ohkita M, Nakajima A, Ueda K, Takaoka M, Kiso Y, Matsumura Y. Preventive effect of flavangenol on ischemia/reperfusion-induced acute renal failure in rats. *Biol Pharm Bull* 2005; **28**: 1655–1657.
9 Sato M, Yamada Y, Matsuoka H, and *et al*. Dietary pine bark extract reduces atherosclerotic lesion development in male ApoE-deficient mice by lowering the serum cholesterol level. *Biosci Biotechnol Biochem* 2009; **73**: 1314–1317.
10 Nakano M, Orimo N, Katagiri N, Tsubata M, Takahashi J, Van Chuyen N. Inhibitory effect of astraxanthin combined with Flavangenol on oxidative stress biomarkers in streptozotocin-induced diabetic rats. *Int J Vitam Nutr Res* 2008; **78**: 175–182.
11 Lee C, Miura K, Liu X, Zweier JL. Biphasic regulation of leukocyte superoxide generation by nitric oxide and peroxynitrite. *J Biol Chem* 2000; **275**: 38965–38972.
12 Lee CI, Liu X, Zweier JL. Regulation of xanthine oxidase by nitric oxide and peroxynitrite. *J Biol Chem* 2000; **275**: 9369–9376.
13 Lee MC, Shoji H, Komatsu T, Yoshino F, Ohmori Y, Zweier JL. Inhibition of superoxide generation from fMLP-stimulated leukocytes by high concentrations of nitric oxide or peroxynitrite: characterization by electron spin resonance spectroscopy. *Redox Rep* 2002; **7**: 271–275.
14 Lee MC, Shoji H, Miyazaki H, and *et al*. Measurement of oxidative stress in the rodent brain using computerized electron spin resonance tomography. *Magn Reson Med Sci* 2003; **2**: 79–84.
15 Lee MC, Shoji H, Miyazaki H, and *et al*. Assessment of oxidative stress in the spontaneously hypertensive rat brain using electron spin resonance (ESR) imaging and *in vivo* L-Band ESR. *Hypertens Res* 2004; **27**: 485–492.
16 Miyazaki H, Shoji H, Lee MC. Measurement of oxidative stress in stroke-prone spontaneously hypertensive rat brain using *in vivo* electron spin resonance spectroscopy. *Redox Rep* 2002; **7**: 260–265.
17 Kobayashi K, Yoshino F, Takahashi SS, and *et al*. Direct assessments of the antioxidant effects of propofol medium chain triglyceride/long chain triglyceride on the brain of stroke-prone spontaneously hypertensive rats using electron spin resonance spectroscopy. *Anesthesiology* 2008; **109**: 426–435.
18 Kuppusamy P, Zweier JL. Cardiac applications of EPR imaging. *NMR Biomed* 2004; **17**: 226–239.
19 Miura Y, Utsumi H, Hamada A. Effects of inspired oxygen concentration on *in vivo* redox reaction of nitroxide radicals in whole mice. *Biochem Biophys Res Commun* 1992; **182**: 1108–1114.
20 Takeshita K, Hamada A, Utsumi H. Mechanisms related to reduction of radical in mouse lung using an L-band ESR spectrometer. *Free Radic Biol Med* 1999; **26**: 951–960.
21 Gomi F, Utsumi H, Hamada A, Matsuo M. Aging retards spin clearance from mouse brain and food restriction prevents its age-dependent retardation. *Life Sci* 1993; **52**: 2027–2033.
22 Miura Y, Ozawa T. Noninvasive study of radiation-induced oxidative damage using *in vivo* electron spin resonance. *Free Radic Biol Med* 2000; **28**: 854–859.
23 van Weelden H, de Gruijl FR, van der Putte SC, Toonstra J, van der Leun JC. The carcinogenic risks of modern tanning equipment: is UV-A safer than UV-B? *Arch Dermatol Res* 1988; **280**: 300–307.
24 Pence BC, Naylor MF. Effects of single-dose ultraviolet radiation on skin superoxide dismutase, catalase, and xanthine oxidase in hairless mice. *J Invest Dermatol* 1990; **95**: 213–216.
25 Takeshita K, Takajo T, Hirata H, Ono M, Utsumi H. *In vivo* oxygen radical generation in the skin of the protoporphyria model mouse with visible light exposure: an L-band ESR study. *J Invest Dermatol* 2004; **122**: 1463–1470.
26 Konaka R, Kasahara E, Dunlap WC, Yamamoto Y, Chien KC, Inoue M. Irradiation of titanium dioxide generates both singlet oxygen and superoxide anion. *Free Radic Med* 1999; **27**: 294–300.
27 Lee JW, Miyawaki H, Bobst EV, Hester JD, Ashraf M, Bobst AM. Improved functional recovery of ischemic rat hearts due to singlet oxygen scavengers histidine and carnosine. *J Mol Cell Cardiol* 1999; **31**: 113–121.
28 Kamibayashi M, Oowada S, Kameda H, and *et al*. Synthesis and characterization of a practically better DEPMPO-type spin trap, 5-(2,2-dimethyl-1,3-propoxy cyclophosphoryl)-5-methyl-1-pyrroline N-oxide (CYPMPO). *Free Radic Res* 2006; **40**: 1166–1172.
29 Lauterbur PC. Progress in n.m.r. zeugmatography imaging. *Philos Trans R Soc Lond B Biol Sci* 1980; **289**: 483–487.
30 Berneburg M, Plettenberg H, Krutmann J. Photoaging of human skin. *Photodermatol Photoimmunol Photomed* 2000; **16**: 239–244.
31 Clifford MN. Diet-derived phenols in plasma and tissues and their implications for health. *Planta Med* 2004; **70**: 1103–1114.

doi: 10.3164/jcbn.10-103